

Preparation, Microstructure, and Thermodynamic Properties of Homogeneous and Heterogeneous Compound Monolayers of Polymerized and Monomeric Surfactants on the Air/Water Interface and on Solid Substrates

W. Frey,[†] J. Schneider,[‡] H. Ringsdorf,[†] and E. Sackmann^{*†}

Physik Department (Biophysics Laboratory E22), Technische Universität München, D-8046 Garching, Federal Republic of Germany, and Institut für Organische Chemie, Universität Mainz, D-6500 Mainz, Federal Republic of Germany. Received August 22, 1986

ABSTRACT: Monolayers of amphiphilic copolymers consisting of two-chain surfactants bridged by hydrophilic chains of various lengths as well as of mixtures of these macrolipids with phospholipids are studied and discussed in terms of the de Gennes-Alexander scaling laws of adsorbed macromolecules. The thermodynamic properties are studied by film balance experiments, and the microstructure is studied by a recently developed phase contrast electron microscopy technique and by electron diffraction. It is demonstrated that heterogeneously organized monolayers of coexisting (fluid or solid) phases of monomeric and polymerized lipid may be transferred from the air/water interface onto solid substrates without structural alterations. Copolymers with long hydrophilic chains exhibit an entropy-driven transition from a two-dimensional expanded into a condensed state with chains confined to a cylinder as predicted by Alexander. The monomer adsorption energy is $-0.1kT$ to $-0.5kT$. The two-dimensional radius of the chains scales as $N^{3/4}$ (N = monomer number) as predicted. Monolayers of the copolymers with long hydrophilic chains swell readily by incorporation of monomeric lipid. The swelling and its saturation behavior are explained in terms of a balance between the entropy of mixing and the entropic elastic free energy associated with the expansion of the hydrophilic chain. The two-dimensional foamlike state of monolayers (gas/fluid coexistence) at low densities is explained in the scaling approach as a counteraction of (1) a hydrophobic repulsion of the hydrocarbon chains from the water surface (repulsion energies $\delta \approx +1kT$ for CH_2), (2) the chain-chain attraction arising since air is a poor solvent, and (3) the translational entropy. The interesting analogy between the swollen copolymer and the two-dimensional networks (the cytoskeleton) of spectrin which is coupled to the inner monolayer of the red cell envelope is pointed out.

Introduction

The introduction of polymerizable amphiphiles into membrane research opens a number of exciting new possibilities for the construction of mechanical models of cell plasma membranes or of models of two-dimensional macromolecular solutions or gels.

The mechanical and dynamic properties of cell plasma membranes are to a large extent determined by the coupling of the lipid/protein bilayer to a quasi-two-dimensional meshwork of protein filaments (such as spectrin and actin in the case of the red blood cell membrane). As described previously,¹ this membrane-associated part of the cytoskeleton plays an essential, although not yet understood, role for shape transformations of cells or for local membrane instabilities associated with chemically induced bending moments.¹⁻³ Thus, local changes in the intrinsic curvature of the membrane appear to trigger many cellular events such as the detachment (exocytosis) and the internalization (endocytosis) of vesicles or the formation of local protrusions (pseudopodia) during cellular migration (e.g., chemotaxis).

In recent experiments² we showed that model membranes composed of macromolecular surfactants (also called macrolipids in the following) and lipid monomers may undergo similar shape transformations as the red blood cell or may display the initial steps of exocytosis and endocytosis. From these model membrane studies it follows that the above-mentioned cellular processes may be understood in terms of general physical principles: the membrane curvature elasticity and chemically controlled intrinsic bending moments (spontaneous curvature). Moreover, these experiments provided evidence that the interconnection of part of the lipids by chains possibly together with lateral phase segregation processes are essential for these processes.

In the present work we investigated monolayers of a new type of macrolipid that consist of two-chain surfactants interconnected by hydrophilic chains, the general structure of which is exhibited in Figure 1. These copolymers are expected to be even more suited for the preparation of mechanical models of cell plasma membranes than the macrolipids studied hitherto. The hydrophilic chains allow for the interaction of monomeric lipids between the amphiphiles and can simultaneously adsorb to the membrane surface. They may thus exhibit the same behavior as the spectrin filaments in the red blood cell which are fixed to membrane-bound proteins at both ends, exhibit a folded structure, and adsorb electrostatically to the charged lipid moiety of the inner monolayer. Macrolipids with charged chains can be easily prepared.

Addition of monomeric lipids to monolayers of the copolymers leads to a swelling of the latter which thus exhibits typical features of a two-dimensional polymer melt. Such mixed monolayers appear to be of general interest as two-dimensional macromolecular solutions in order to test scaling laws.⁴

A further purpose of the present work is to demonstrate for the first time that heterogeneously organized monolayers composed of (fluid or solid) patches of macrolipid and of monomeric lipid, respectively, may be disturblessly transferred from the air/water interface onto solid substrates. Such ultrathin and partially polymerized films are hoped to promote the application of Langmuir-Blodgett films in microelectronics^{5,6} for the preparation of biosensors,^{5,7} and the buildup of organized molecular assemblies⁸ or in order to render surfaces biocompatible.⁹ During the past years a large number of different types of polymerizable amphiphiles have been synthesized (cf. ref 9-18), and it has thus become possible to prepare partially polymerized lipid lamella with a variety of physicochemical properties for such purposes.

In the second half of this paper the properties of pure and mixed monolayers are discussed in terms of the scaling-law theory of adsorbed macromolecules of de

* Author to whom correspondence should be addressed.

[†] Technische Universität München.

[‡] Universität Mainz.

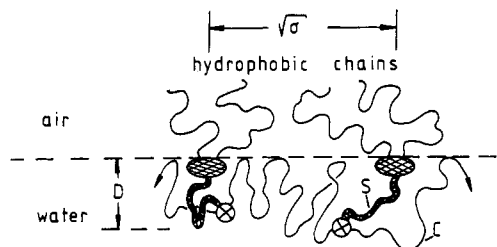


Figure 1. Schematic view of macrolipid composed of amphiphilic molecules carrying hydrophilic spacers (S) that are interconnected by hydrophobic chains (C). The copolymer is fixed at the air/water interface. The hydrophilic layer thickness is D , and σ is the average area per amphiphilic molecule. Thus $\sigma^{1/2}$ is the average distance between nearest-neighbor amphiphiles.

Gennes^{20,21} and Alexander²² where the hydrophilic chain corresponds to the adsorbed macromolecule and the amphiphatic part serves to anchor the first to the surface. Although in the present case both ends of the chain are confined to the surface, many properties can at least be explained semiquantitatively by these models.

Material and Methods

Materials.²⁵ The phospholipids, DMPC and DMPE, were obtained from Fluka and were used as purchased.

The polymerizable phosphate (I) abbreviated as (4,16)-PO-MECY (where the first digit (4) stands for the number of $\text{CH}_2\text{-CH}_2\text{O}$ groups and the second (16) for the number of C atoms of the hydrocarbon chain synthesized as described elsewhere¹⁴). The thermodynamic and structural properties of bilayers of this lipid as well as of mixtures with DMPC were reported previously.

The monomeric lipids were polymerized in a toluene/dioxane (1:1) mixture with 1 mol % 2,2'-azobis(isobutyronitrile) (AIBN) as radical initiator. After the mixture was flushed with nitrogen at 20 °C for 15 min, the polymerization was carried out at 65 °C and the mixture was kept for 10 h at this temperature for *homopolymerization* and for 5 h for *copolymerization* (conversion about 50%). The polymeric lipids were precipitated in a suitable solvent (methanol, acetone) and vacuum-dried from benzene. The polymers were characterized by thin-layer chromatography and ¹H NMR spectroscopy. The composition of the statistical copolymers was determined by microanalysis.

Film Balance and Monolayer Transfer. Monolayers are prepared by spreading solutions of the lipids or the lipid mixtures on the air/water interface of a film balance (Wilhelmy-type measuring system) described previously.²⁴ The solvent is 3:1 chloroform-methanol and the lipid concentration about 0.5 mg/mL. The water in the subphase is purified by distillation and passed through a Millipore filtration system. For the electron microscopic studies the monolayers are deposited onto electron transparent substrates²³ by pulling the latter out from the water subphase at a speed of 0.34 cm min⁻¹ by using a film lift. During this procedure the lateral pressure is held constant automatically by controlling the position of the barrier.

The sandwich-type substrate is made up of three subsequent layers of (1) Formvar (Merck, Darmstadt, FRG) of 200-Å thickness, (2) carbon (50 Å), and (3) SiO (50 Å). The Formvar film is prepared by dipping a glass slide into a Formvar-chloroform solution using a film lift. After drying, the thin film is scaled from the glass onto an air/water interface. Subsequently, the latter two layers are vacuum deposited at 10⁻⁶ mbar. In order to enable observations by transmission electron microscopy, the sandwich-type substrate is deposited onto electron microscope grids. In order to avoid destruction of the monolayer during the transfer procedure, one or several substrate-covered grids are originally deposited onto glass microslides (2.4 × 2.4 cm²). In this way the danger of a disruption of the monolayer by surface tension effects (during the drying of the deposited film) is minimized.²³ It should also be pointed out that the substrate has to be used within hours after preparation in order to avoid the SiO surface becoming hydrophobic.

For the electron microscopy a Phillips EM 400 T microscope is used. The phase contrast micrographs are taken in the low-magnification mode by defocusing (underfocus) between 1 cm

(magnification < 800×) and 0.125 cm (> 800×). The physical basis of the contrast formation by charge decoration has been described in detail previously.²³ In order to minimize radiation damage, the low-dose unit is used in particular for the exposures.

The electron diffractions are taken with the selected-area technique of Rieke²⁶ which enables us to take diffractions from small sample areas down to 3 μm². Such experiments are possible with the EM 400 T equipped with a twin-objective lens.

Most of the samples are simultaneously studied by the low-angle platinum shadowing technique and by scanning transmission electron microscopy (STEM) in order to check the homogeneity of the deposited monolayers and to determine approximate thickness differences of different monolayer phases. As shown previously,^{23b} quantitative information concerning the lipid-packing density can be obtained by the density-mapping method using STEM.

The platinum shadowing is performed in a Balzers BAF 400 D device under an angle of incidence of $\alpha \approx 15^\circ$ at 10⁻⁶ mbar. Pt layers of 10–12-Å thickness are deposited. Thickness differences, h , are estimated from the shadowing lengths, s , according to $h = s \tan \alpha$. Normally the same sample is simultaneously studied by all three techniques with the platinum shadowing being performed after completion of the phase contrast and scattering experiments.

Experimental Results

Pressure-Area Diagrams of Macromolecular Lipids. In Figures 2 and 3 we present a series of isotherms of the copolymers composed of two-chain surfactants connected by hydrophilic chains that exhibit the general structure shown in Figure 1. Isotherms of two types of copolymers with different lengths of the hydrophilic chain, C , and structures of the surfactant, respectively, are compared. In addition, Figure 4a shows the isotherm of the polymerized lipid of structure I with no hydrophilic chain C .

The isotherms exhibit the following characteristic features. (1) For short hydrophilic chains ($z = 0-2$) one observes the same pronounced phase transition from a two-dimensional fluid to a two-dimensional solid (condensed) state as for normal surfactants. The transition pressures π_m increase with increasing temperature as predicted by the Clausius-Clapeyron equation for exothermic fluid-to-solid transitions.^{24a} (2) If the total length of the hydrophilic chain (consisting of the monomers from the spacer S and of the hydrophilic chain C , respectively; cf. Figure 1) is increased ($z \geq 5$), the form of the isotherm changes in a characteristic way: First, the limiting molecular area A_{om} (cf. Figure 2 for definition) below which a lateral pressure starts to build up is shifted to very large areas and increases with the hydrophilic chain length. Second, the isotherms exhibit a remarkable break at a pressure π_b (which is indicated in Figures 2 and 3 by arrows) above which the slope of the isotherms decreases. This strongly suggests a transition from an expanded to a condensed state. It is very noteworthy, however, that the pressure π_b of the isotherms is nearly temperature independent or is slightly shifted to lower pressures with increasing temperature. If we interpret the break as a phase transition, as will be done below, this means that the Clausius-Clapeyron coefficient $d\pi_b/dT = \Delta S/\Delta A$ is negative, where ΔA and ΔS are the changes in area and in entropy, respectively, at the transition from the expanded to the condensed state. Normal behavior ($d\pi_b/dT > 0$) is observed if the monolayer is further condensed. In fact, a change in the sign of $d\pi_b/dT$ occurs at about the same area ($A \approx 120 \text{ Å}^2$) for all copolymers.

Microstructure of Monolayers. In order to get insight into the microscopic structural changes of the lipid monolayer caused by the lateral compression we present in the following a number of electron microscopic studies

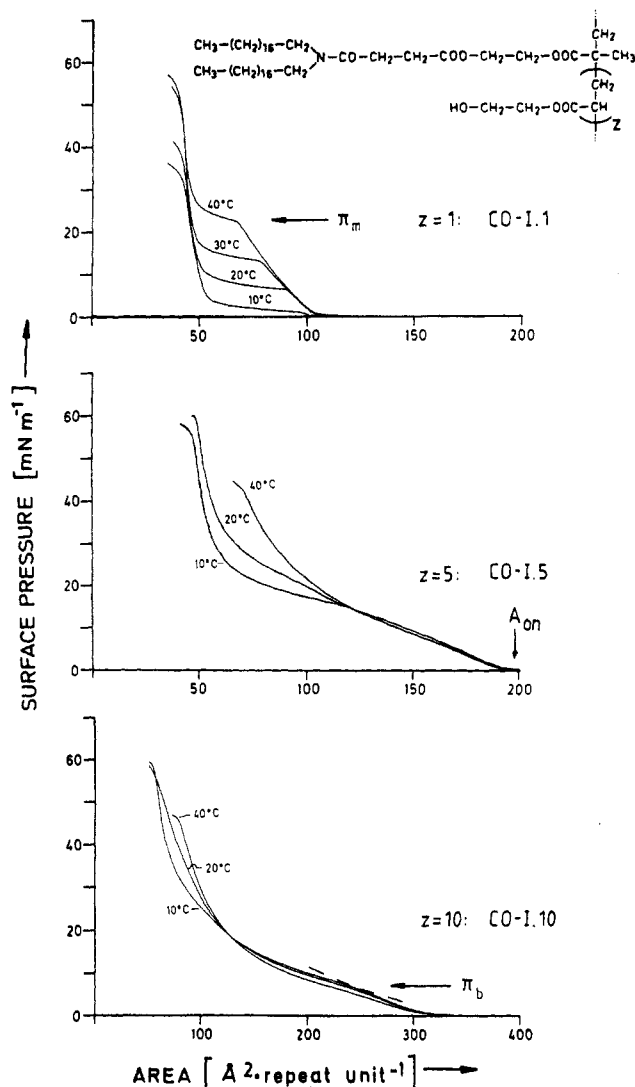


Figure 2. Isotherm of copolymer (CO-I, z) of the structure shown in the figure with increasing length of hydrophilic chain from top to bottom. z denotes the ratio of the number of hydrophilic $\text{CH}_2\text{CHCOOCH}_2\text{CH}_2\text{OH}$ groups to the number of surfactants: (top) $z = 1$; (middle) $z = 5$; (bottom) $z = 10$. Isotherms for the different temperatures indicated are given. π_m denotes the transition pressure of the chain melting transition and π_b the pressure at which the copolymers with long hydrophilic chains exhibit a break. The abscissa are given in units of square angstroms per amphiphile; note the different scale of the bottom curve.

of the monolayers deposited onto the electron transparent substrates. Since we intend to demonstrate simultaneously that heterogeneously organized monolayers composed of polymerized and monomeric lipid domains (of which one at least is fluid) may be transferred disturblessly from the air/water interface to solids we present (with the exception of Figure 4) results for mixtures of polymerized and unpolymerized lipids. Here we report only results with DMPE as the monomer because with this component we managed to prepare the most stable monolayers. With other phospholipids—in particular synthetic lecithins—the transferred monolayers tend to exhibit cracks and holes which are attributed to a reorganization after transfer such as local crystallization. This holds especially for lipids forming crystalline phases with collectively tilted chains, such as DMPC.

Figure 4 shows first an example of a binary mixture of monomers: DMPE and *m*-(4,16)-POMEYCY. The lipids exhibit fluid-to-solid transitions at different transition

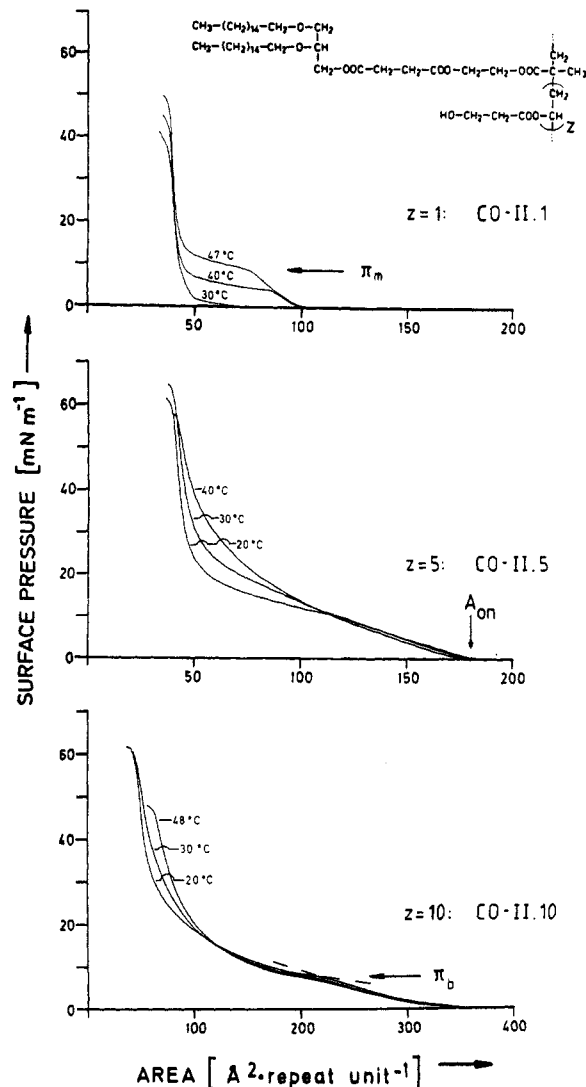


Figure 3. Isotherms of copolymer CO-II, z of the structure shown in the figure: (top) $z = 1$; (center) $z = 5$; (bottom) $z = 10$. The temperatures are indicated at the curves.

pressures. The breaks in the isotherms (some are indicated in Figure 4a by arrows) correspond to discontinuities in the lateral compressibilities and thus indicate the phase boundaries of the mixed monolayer from which the phase diagram could in principle be established.^{24a} At the break of curve b (at arrow in Figure 4a), for example, lateral phase separation into a crystalline phase of nearly pure DMPE and a fluid phase poor in this component occurs.

This phase separation is clearly demonstrated by the phase-contrast electron microscopy and diffraction experiments shown in Figure 4b. In the phase-contrast micrograph, dark dendrite-like platelets appear at pressures above the break point which grow in size with increasing pressure. They exhibit sharp hexagonally arranged diffractions (inset of Figure 4b), demonstrating that the platelets are two-dimensional monocrystals.²⁴ The region between the platelets exhibits only diffuse diffraction rings. In contrast, it follows from platinum shadowing experiments that these regions are also covered by a monolayer which is obviously in an amorphous phase and which consists of nearly pure *m*-(4,16)-POMEYCY. The phase-contrast difference is attributed to a higher electric charging of the crystalline DMPE domains.²³

Figures 5 and 6 show two examples of mixed monolayers of the polymeric lipid without hydrophilic chain, namely, *p*-(4,16)-POMEYCY with two types of monomeric lipids:

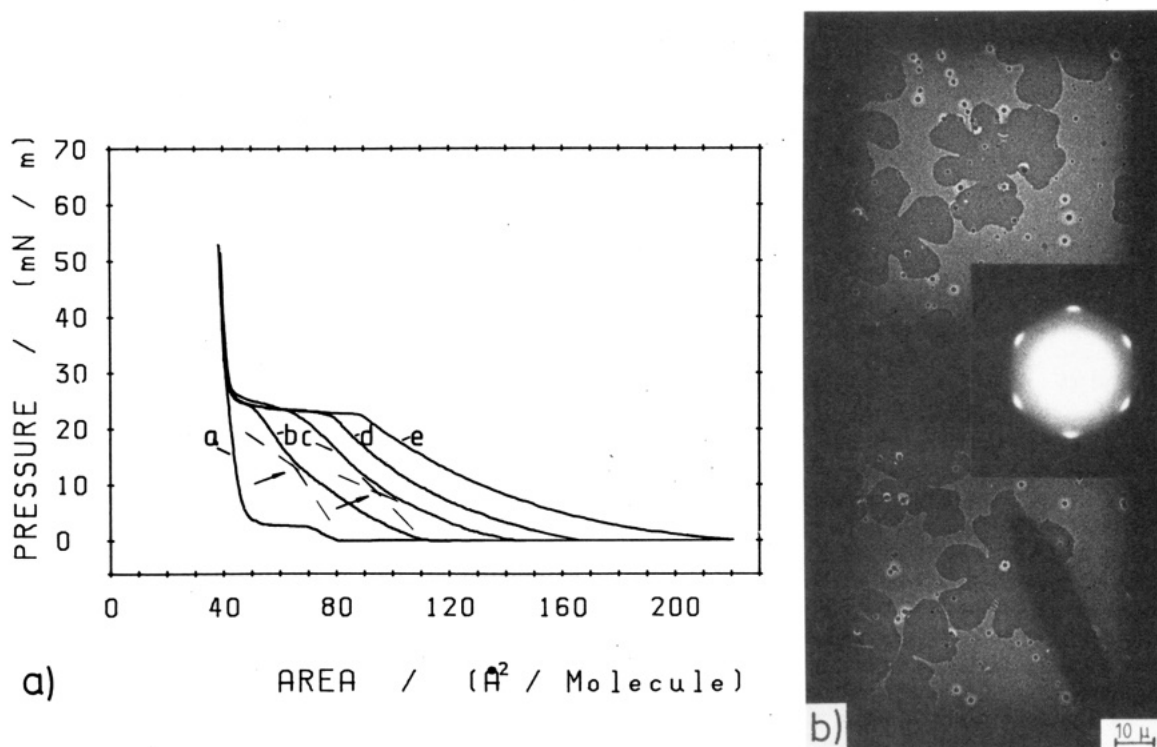


Figure 4. (a) Isotherm of mixture of monomers, namely, monomeric (4,16)-POMECEY and DMPE at 20 °C. The molar fractions of DMPE are (a) $x_E = 1.0$, (b) $x_E = 0.75$, (c) $x_E = 0.5$, (d) $x_E = 0.25$, (e) $x_E = 0.0$. Arrows indicate liquidus lines of mixtures. (b) Phase-contrast micrograph of mixture containing 75 mol % DMPE and transferred from 18 m^{-1} (cf. circle in a), that is, from the fluid–solid coexistence region. Inset: electron diffraction pattern of dark dendrite-like domains.

DMPE (Figure 5) and *m*-(4,16)-POMECEY (Figure 6). These systems were chosen because the chain-melting transition of the macrolipid is in one case higher (Figure 5) and in the other lower (Figure 6) than the monomer phase change, enabling the preparation of monolayers of coexisting patches made up of solid macrolipid and of fluid monomeric lipid, respectively, and vice versa. As has been established in separate experiments, these compound monolayers can also be prepared by photopolymerization of the POMECEY on the air/water interface.

The interesting conclusions following from Figures 5 and 6 are the following. (1) Continuous monolayers of coexisting fluid and solid phases may be deposited on solids in both cases. One of the phases is a two-dimensional polymer melt (fluid in Figure 5 and solid in Figure 6) and the other a solution of the macrolipid in the monomer. (2) The mixture of DMPE and *p*-POMECEY behaves as a eutectic system since the onset of the transitions of both DMPE and *p*-POMECEY are shifted to higher pressures if the second compound is added. (3) Polymerization leads to a strong shift of the phase transition to lower pressures (corresponding to higher temperatures), which strongly suggests that its causes condensation of the monolayer. This is a consequence of the restriction of the freedom of motion of the hydrophilic head groups.

Figures 7 and 8 summarize some important results concerning the microstructure of the copolymer COP-II,10 together with mixtures of this lipid with DMPE. The transfer pressures are indicated in the isotherms of Figure 7a.

Figure 7b shows a phase-contrast electron micrograph of a monolayer of the pure copolymer transferred from a pressure (S in Figure 7a) slightly above the break (at π_b) of the isotherm. Small dark platelets are observed. These grow in number and size and merge at increasing pressure and finally exhibit a crystal-type electron diffraction pattern. This provides strong evidence that the monolayer

condensation at π_b is associated with a crystallization of the hydrophobic chain region. This would imply a collective tilting of the hydrocarbon chains in order to allow for a tight packing of the chains. Direct evidence for such a tilting is also provided by the finding of Figure 7c that the monolayer transferred at a high pressure (34 mN m^{-1} ; point R in Figure 7a) exhibits a corrugated (rippled) surface profile with amplitudes of about 25 Å. Chain tilting is indeed expected for all lipids that exhibit very large head groups such as is the case for the copolymer.

As is demonstrated in Figure 8, continuous monolayers made up of mixtures of the copolymer with DMPE can be transferred onto solid substrates at all compositions. In this case two-dimensional single crystals of nearly pure DMPE form at lower pressures; the crystals increase in number but not very much in size with increasing pressure. At further increasing pressures the copolymer crystallizes as well. In Figure 8c it is demonstrated that the monolayer deposited from the completely condensed state is homogeneous. However, this is also the case for films transferred from the fluid–solid coexistence. The circular DMPE domains are about 15 Å less thick than the intermediate regions, which is indeed expected since the thickness of the DMPE is determined by the hydrocarbon chains and that of the polymeric lipid by both the hydrophobic and the hydrophilic chains.

Swelling of the Copolymer. Figure 7a exhibits another interesting behavior of the copolymer monolayer that is of more general interest. The DMPE readily dissolves in the fluid monolayer of the copolymer up to about an equimolar composition of the two types of surfactants. Further addition of DMPE leads to decomposition of the monolayer into the saturated phase and the nearly pure DMPE. This conclusion is suggested by the finding that above the saturation point DMPE crystallizes at about the same pressure as the pure compound. In contrast, the transition pressure π_b of the expanded-to-condensed phase

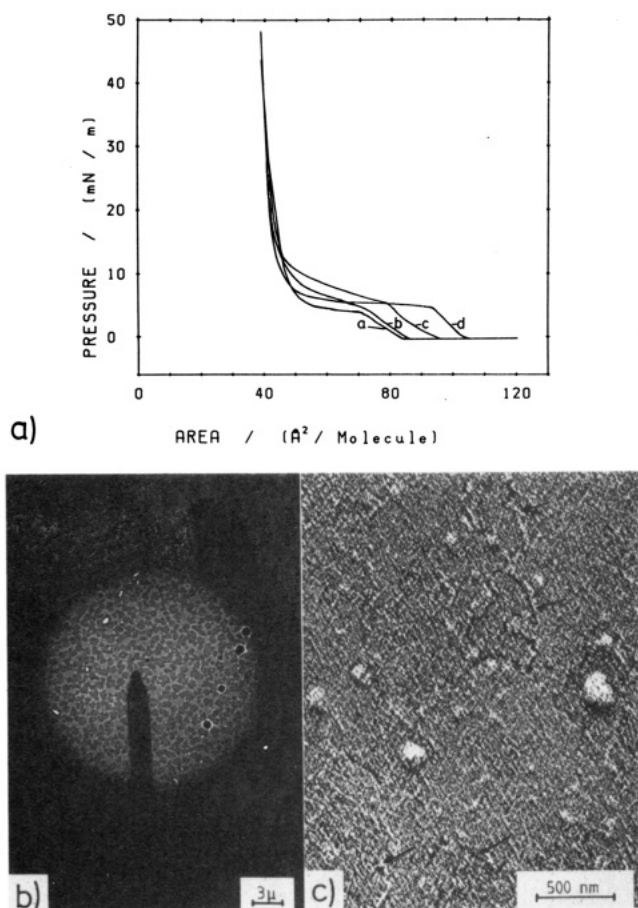


Figure 5. (a) Isotherms of mixture of homopolymeric lipid *p*-(4,16)-POMECEY with monomeric lipid DMPE taken at 20 °C. The molar fractions of DMPE are (a) $x_E = 1.0$, (b) $x_E = 0.75$, (c) $x_E = 0.5$, (d) $x_E = 0.0$. (b) Phase-contrast electron micrograph of monolayer of 1:1 mixture transferred from 7 mN m⁻¹. (c) Dark field scanning transmission electron micrograph of same monolayer as in (b) after platinum shadowing. The small platelets indicated by short arrows correspond to the dark precipitates (one is marked by dashed contour line).

change of the copolymer is only shifted to a slightly lower value by the swelling. The circular precipitates formed at π_b (cf. Figure 8b) are probably made up of the condensed copolymer containing DMPE. At higher pressures ($\pi > 30$ mN m⁻¹) a recrystallization occurs, leading to decomposition into the two nearly pure crystalline components.

Below, the swelling is explained in terms of a balance between the gain in free mixing energy and the expense in entropic elastic free energy associated with the expansion of the hydrophilic chains.

Discussion

Introductory Remarks. As compared to normal amphiphiles, the monolayers of surfactants connected by hydrophilic chains exhibit the following new properties. (1) A lateral pressure arises at very large molar areas. The area, A_{on} , of this pressure onset increases strongly with increasing hydrophilic chain length. (2) Copolymers with long hydrophilic chains exhibit a pronounced transition from an expanded to a condensed state, exhibiting at least a short-range crystalline order. The transition pressure, π_b , decreases slightly with increasing temperature ($\Delta\pi_b/\Delta T < 0$), which suggests that the condensation transition is an entropy-driven process. A crossover to a regime with normal behavior ($\Delta\pi/\Delta T > 0$) is observed at an area of about 120 Å² for all copolymers. (3) Monolayers made up of copolymers with long hydrophilic chains can dissolve

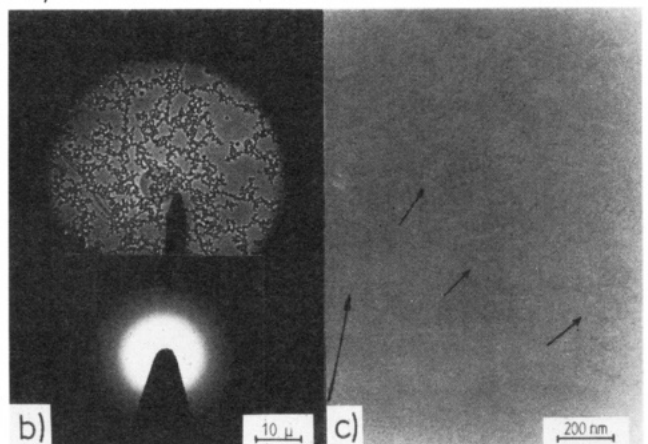
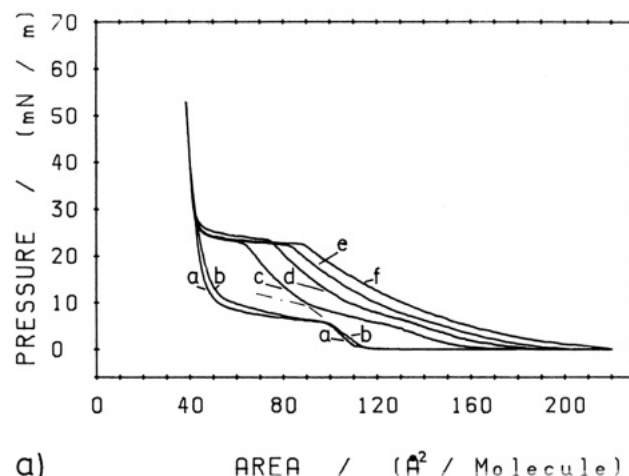


Figure 6. (a) Pressure-area curves at 20 °C of the polymerized surfactant *p*-(4,16)-POMECEY of structure I and of mixtures of this lipid with the unpolymerized component are shown for different compositions: (a) pure polymer ($x_m = 0.0$); (b) molar fraction of unpolymerized component $x_m = 0.1$; (c) $x_m = 0.5$; (d) $x_m = 0.75$; (e) $x_m = 0.9$; (f) pure monomer ($x_m = 1.0$). Note that x_m is equal to the number of monomeric lipids to the total number of monomeric and polymerized surfactants. (b) Phase-contrast electron micrograph and electron diffraction pattern of monolayer of 1:1 mixture transferred on substrate from a pressure of 21 mN m⁻¹ where a fluid *m*-POMECEY-rich phase coexists with crystalline *p*-POMECEY. Simultaneously the diffraction pattern of this phase is given. (c) Platinum shadowing of above monolayer. The small platelets (short arrows) correspond to the dark precipitates of Figure 5b. Arrow indicates shadowing direction.

large quantities of monomeric lipid by swelling. The swelling is associated with an expansion of the hydrophilic chain and exhibits saturation behavior.

The above summary of unique properties of the monolayers of copolymeric lipids suggests that at large expansions their behavior is determined by the adsorption of the hydrophilic chain to the interface and in the completely compressed state (<120 Å²) by the interaction of the hydrocarbon chains.

In the following we provide evidence that the special features of the copolymers can be understood in terms of the scaling theory of adsorbed macromolecules of de Gennes^{4,20,21} and Alexander.²² Moreover, the transition to a two-dimensional foam above the area (A_{on}) of the pressure onset, which is characteristic for all surfactants,^{24,26} is explained in terms of the scaling approach.

The adsorbed macromolecular layers are characterized by the following parameters: (1) N , the degree of polymerization, which in our case is assumed to be equal to the number of monomers of one hydrophilic spacer (S ; Figure 1) and of the connecting chain (C ; Figure 1); (2) D , the thickness of the adsorbed macromolecular layer, which in

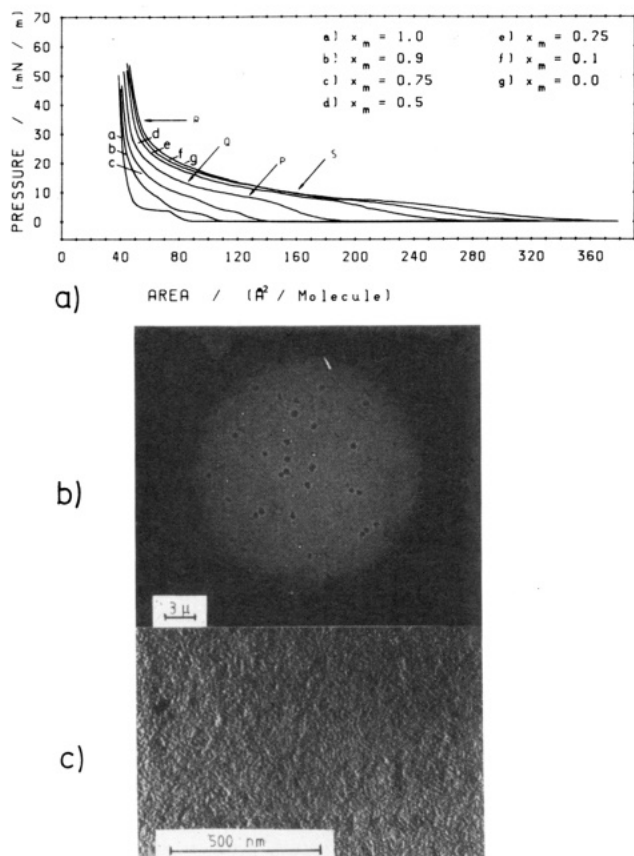


Figure 7. (a) Isotherm of mixture of copolymer COP-II,10 of Figure 3 with DMPE taken at 20 °C. The molar fractions of DMPE (x_m) are given in the figure. x_m is equal to the ratio of the number of DMPE molecules to the total number of surfactants (DMPE and polymerized lipid). (b) Phase-contrast electron micrograph of pure COP-II,10 monolayer transferred from pressure (10 mN m⁻¹) slightly above the break of the isotherm (S, in Figure 7a). The dark spots grow in size with increasing pressure, and the monolayer exhibits a crystalline diffraction pattern that vanishes, however, very rapidly. (c) Micrograph of platinum-shadowed monolayer of pure COP-II,10 transferred at high pressure (R, in (a)). Clearly, a closed film results that exhibits, however, a wavy surface profile.

our case consists always only of one chain; (3) δ , the interaction energy of one monomer (in units of $k_B T$) with the interface ($\delta < 0$ for attraction); (4) σ , the average area per surfactant (or polar head) of the copolymer, so that $\sigma^{1/2}$ is the average distance between neighboring surfactants and the number density, c , of monomers (per cubic centimeter) is given by $N/\sigma D$; (5) a , the dimension of one monomer.

According to Daoud and de Gennes^{20,21} and Alexander,²² the behavior of adsorbed polymers is determined by the balance of the following interactions: (1) the adsorption of the hydrophilic chain to the interface, which is determined by the fraction of monomers (a/D) in contact with the surface, so that the free energy of adsorption per chain is given by

$$f_{ad} \approx -kT\delta N(a/D) \quad (1)$$

(2) the interaction between the monomers, which is repulsive since the water is a good solvent, so that the free energy per chain is

$$f_{rep} \approx kT \frac{a^3 N^2}{D\sigma} \quad (2)$$

(In order to simplify the discussion the Flory-Huggins approximation is used instead of the correct scaling law approach ($f_{rep} \propto (N/\sigma D)^{5/4}$) since the difference of the

exponents (1.0 instead of 1.25) is outside of our experimental accuracy.) (3) the loss in entropy resulting from the confinement of the chain, which is brought about by its adsorption to the surface and which accounts for the entropic elasticity of the chain.

$$f_{el} \approx N(a/D)^{5/3} \quad (3)$$

In the scaling approach all numerical coefficients are ignored, which is indicated in eq 1–3 by using the equivalence symbol (\approx) instead of the equal sign. Finally, one has to account for the translational entropy of the two-dimensional arrangement of amphiphiles. The free energy per chain is

$$f_{trans} = kT \ln \sigma \quad (4)$$

Up to pressures of about 40 mN m⁻¹ (where the monolayers start to collapse), the copolymers can be treated as completely insoluble in the aqueous phase at least in the time scale of several hours in which our experiments are performed. Moreover, the molar area is changed so slowly ($A/t = 0.5$ cm²/s⁻¹) that an optimal thickness D can adjust for each value of the molar area σ . Thus the equilibrium thickness, D , is determined by minimizing the total free energy: $f = f_{ad} + f_{rep} + f_{el} + f_{trans}$. The free energy can then be expressed in terms of N and σ .

Hydrophilic Chain Length Dependence of Onset Pressure. Starting at the low-density limit a finite lateral pressure will begin to build up if the area is reduced to such an extent that the hydrophilic chains start to interpenetrate. This occurs if the area per surfactant, σ , becomes equal to the square of the two-dimensional Flory radius, R_{F2} , of the hydrophilic chain. According to Daoud and de Gennes²¹ the latter is given by

$$R_{F2} = aN^{3/4}(a/D)^{1/4} \quad (5)$$

and therefore the following power law follows for the onset area by minimizing f with respect to D :

$$A_{on} = a^2 N^{3/2} \delta^{3/4} \quad (6)$$

This scaling law appears to be well fulfilled if copolymers of similar structure are compared. In Figure 9 the onset areas of the copolymers of Figures 2 and 3 are plotted as a function of $N^{3/2}$. A linear relationship is indeed found that fits the data certainly better than the linear power law $A_{on} \propto N$. Remarkably, the onset area of the homopolymer *p*-POMECEY is in good agreement with the value predicted by eq 6.

From the slope of the straight line in Figure 9 the monomer interaction energy can be estimated. For a value of the monomer dimension of $a = 5$ Å² one obtains $\delta \approx -0.1kT$.

Area Dependence of Surface Pressure. In Figure 10 a double-logarithmic plot of the isotherm of the copolymer CO-II.10 is presented. Two straight-line regions are clearly observed: one at pressures below the break point $\pi_b = 7$ mN m⁻¹ (200 Å² $\leq A \leq 280$ Å²) and one that extends to rather small areas ($A \geq 60$ Å²). These define regimes of different power laws, namely,

$$\pi - \sum_0 \propto \sigma^{-1} \quad \text{for } \pi > \pi_b$$

and

$$\pi - \sum_0 \propto \sigma^{-4.6} \quad \text{for } \pi < \pi_b$$

where \sum_0 is the surface pressure of a pure-water surface.

The power laws predicted by the scaling approach depend, on the regime considered. For very low densities where the chains are well separated a linear relationship $\pi - \sum_0 \propto \sigma^{-1}$ is expected. But this case is not realized in monolayers which do not form a two-dimensional gas but

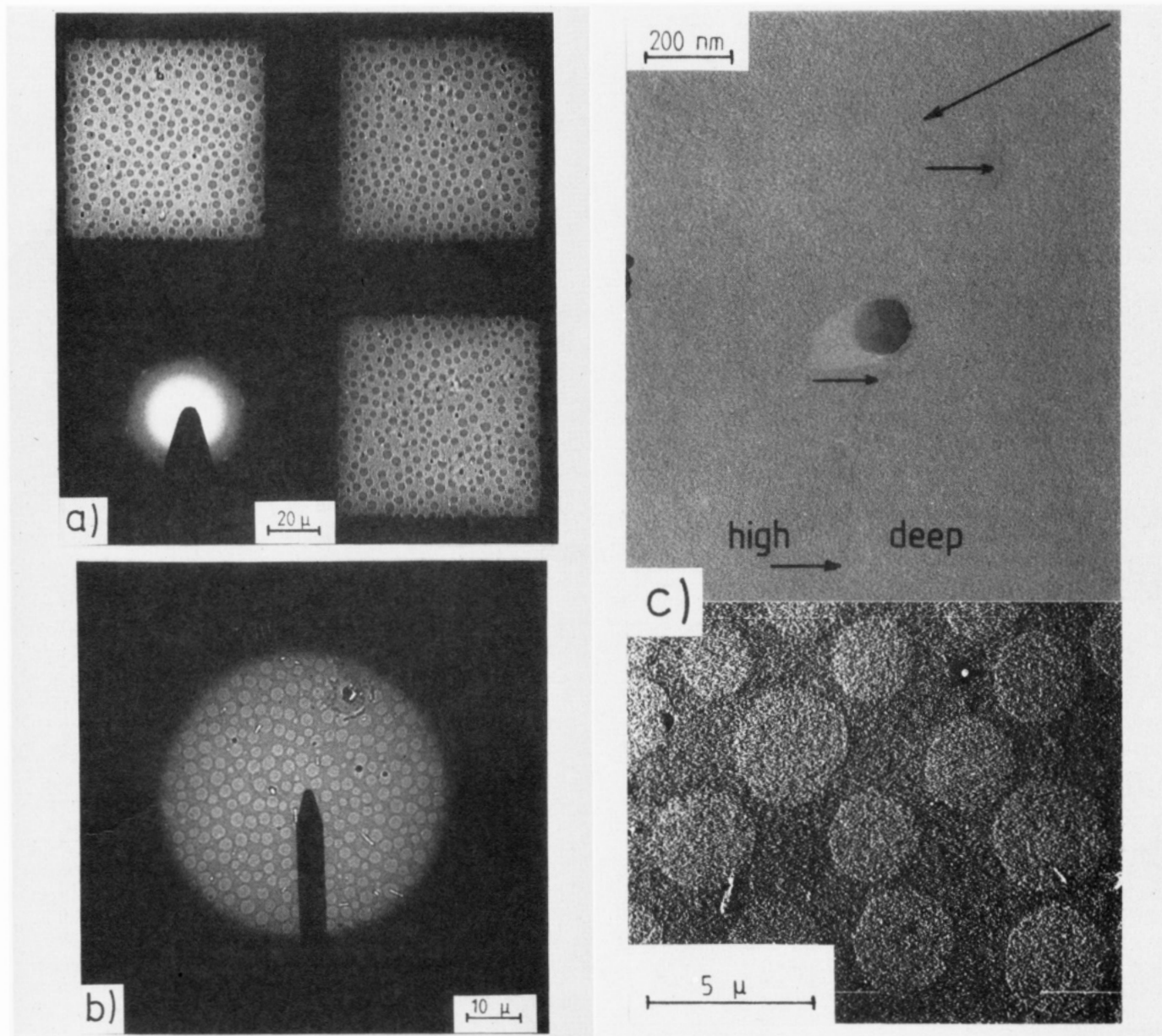


Figure 8. (a) Phase-contrast electron micrographs of 1:1 mixed monolayer of copolymer COP-II,10 with DMPE transferred at 20 °C from 13 mN m⁻¹ (Q in Figure 4a). Inset shows diffraction pattern. (b) Phase-contrast electron micrograph and diffraction pattern of monolayer at 35 mN m⁻¹. (c) Demonstration of continuity of monolayer of 1:1 mixture transferred at 35 mN m⁻¹ by dark field scanning transmission (STEM; bottom) and platinum-shadowing experiment (top). Arrows indicate boundaries between two phases. Long arrow indicates shadowing direction. The height difference of the two phases is about 15 Å (shadowing angle 15°).

a foamlike state up to very large areas ($\sigma > 1000 \text{ Å}^2$).

At densities where the hydrophilic chains overlap, the power law depends on the adsorption energy δ : (1) For strong adsorptions the law for the two-dimensional semidilute regime holds^{20,22}

$$\pi - \sum_0 \propto \sigma^{-3} \quad (7)$$

which corresponds to the highest power predicted. (2) For weak adsorption (when the chains are removed from the surface during the compression) the monolayer exhibits again a softer power law

$$\pi - \sum_0 \propto \sigma^{-11/6} \quad (8)$$

At first sight the scaling law predictions seem to disagree with the experiment. In contrast, the exponent at large areas (near A_{on}) depends very critically on the assumption concerning the pressure of the foamlike state $A > A_{\text{on}}$. This has been assumed as zero, which is not correct since the two-dimensional gas coexisting with the condensed patches will certainly exhibit a finite surface pressure. In

fact, a pressure of about 1 mN m⁻¹ of the foam state would decrease the exponent from $m = -4.6$ to $m = -3$, which is in agreement with eq 7. A pressure of 1 mN m⁻¹ would correspond to an area per molecule of $\sigma = 500 \text{ Å}^2$ in the gas state. This is a reasonable value since ellipsometric and electron microscopic (mass density mapping) experiments performed in our laboratory provided evidence that the gas-state density is only by about a factor of 5 smaller than that of the condensed state at the onset pressure A_{on} .^{23c}

Expanded-to-Condensed Phase Transition. The transition of the copolymers at the break point π_b exhibits two interesting features: (1) it occurs at remarkably large areas (200 Å² for $z = 10$) and (2) it exhibits an anomalous temperature dependence. Since it is accompanied by a crystallization of the hydrophobic chains it is considered a first-order transition.

A first-order transition from an expanded two-dimensional regime with significant surface attraction (δ) to a high-density state in which the hydrophilic chains are

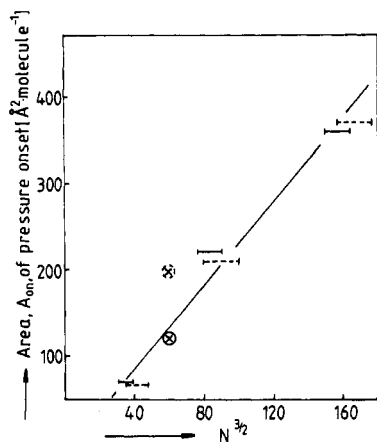


Figure 9. Limiting area, A_{on} , (onset area) below which a lateral pressure starts to build up is plotted as a function of the degree of polymerization, N (equal to number of monomers in the spacer, S , of one surfactant and of the hydrophilic chain, C) to the power $3/2$ for copolymers of Figures 2 and 3: (—) COP-II with $z = 1-10$; (---) COP-I with $z = 1-10$. The point corresponds to monomeric (4,16)-POMECY and x to the polymerized compound.

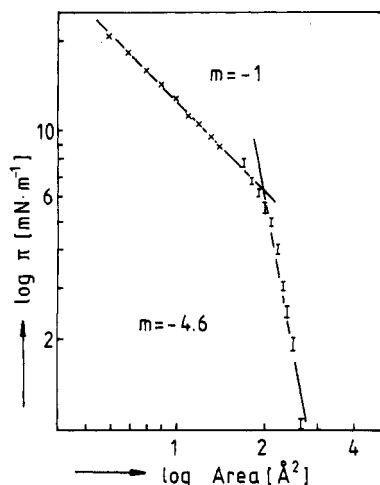


Figure 10. Double-logarithmic plot of lateral pressure vs. area per molecule for the copolymer CO-II,10. The crossover between the two straight-line regions occurs at $A = 200 \text{ Å}^2$.

stretched perpendicular to the membrane surface (δ non-significant) was indeed predicted by Alexander.²² Since the area change is $\Delta A < 0$, the very small negative value of $d\pi_b/dT$ is due to a small increase in total entropy ΔS at the expanded-to-condensed phase transition. Since it is accompanied by a crystallization of the hydrocarbon chains ($\Delta S_{\text{melt}} \approx -10 \text{ cal K}^{-1} \text{ M}^{-1}$) the change in the hydrophilic chain configuration must provide a correspondingly large positive entropy change ΔS_c . It may be estimated from the difference in free energy per chain between the expanded state with a pancake-like structure of the hydrophilic chain and the condensed state where the chains exhibit a brush like configuration. According to eq 2.20 and 2.11 in ref 22 it follows

$$\Delta S_c \approx -kN(\sigma^{-5/6} - \delta^{5/2})$$

The degree of polymerization of the copolymer with the longest hydrophilic chain is $N = 30$, and the molecular area is $A \approx 150 \text{ Å}^2$ (or $\sigma = 10$ since $a^2 = 16 \text{ Å}^2$). In order to compensate the melting entropy the surface attraction energy would therefore have to be $\delta \approx -0.5kT$, which appears to be a reasonable value. In view of the fact that all numerical coefficients are ignored this is only an order of magnitude estimation. It shows, however, that the condensation transition at π_b can well be an entropy-driven process.

It should be noted that an additional possibility contributing to the entropy increase at the expanded-to-condensed transition is a reversible transfer of amphiphiles from the monolayer to the aqueous phase. Such a mechanism has been postulated to be responsible for anomalous polymer adsorption isotherms showing increasing adsorption from the solution with increasing temperatures.²⁸ Such a mechanism is, however, rather unlikely for monolayers of the pure copolymers since the solubility of this type of macrolipid in water is extremely small.

Swelling of Two-Dimensional Copolymer and Saturation Behavior. As follows from Figure 7a copolymers with large hydrophilic chains can incorporate large amounts of monomeric lipids (for instance, up to 50 mol % DMPE) without affecting the expanded-to-condensed phase transition. They thus exhibit the same type of swelling as ordinary three-dimensional gels. One interesting aspect of the swelling of the two-dimensional macrolipid is the saturation behavior which follows from the finding that above about 50 mol % DMPE two clearly separated transitions are observed instead of a broad transition region characteristic for continuous-phase separation at increasing (or decreasing) pressure. The two phases, that is, the nearly pure DMPE and the copolymer saturated with DMPE, appear to behave as two independent fluid monolayers below the transition pressure of the monomeric lipid.

The swelling and saturation behavior can be understood by combining the scaling concept with the regular solution theory. It is obviously determined by the balance of several forces: (1) The driving force for swelling is the entropy of mixing of the two kinds of amphiphiles. (2) The swelling leads to an increase in the average distance, $\sigma^{1/2}$, between the amphiphiles of the macrolipid. The entropic elastic energy associated with the stretching of the hydrophilic (adsorbed) chain opposes swelling. (3) The swelling behavior is further modulated by the interaction of the hydrophilic chain with the interface. If the interaction of this chain with the head group of the monomer was higher than with a free water surface, swelling would be favored and vice versa. Particularly strong effects are expected for charged lipid monomers and hydrophilic chains.

In order to simplify the following more quantitative discussion we ignore the adsorption free energy and discuss its influence at the end. Furthermore, the hydrophilic chain is considered to behave ideally, so that the elastic free stretching energy is given by $f_{el} = \frac{3}{2}kT(\sigma/R_0)^2$. The ideal free energy of mixing is $f_{\text{mix}} = x_1 \ln x_1 + x_2 \ln x_2$, where x_1 and x_2 are the molar fractions of the lipid monomer (x_1) and the polymerized surfactant (x_2).

In order to find the relationship between the length $\sigma^{1/2}$ and the degree of swelling it is useful to introduce the molar ratio $m (=x_1/x_2)$ of the total number of monomers to the total number of polymerized surfactants, so that $x_1 = m/(1+m)$ and $x_2 = 1/(1+m)$. The average distance between two polymerized surfactants (and thus the length of the hydrophilic chain) can then be related to the molar ratio m by

$$\sigma^{1/2} = l_0(1+m)^{1/2}$$

where l_0 is the average cross section of the two amphiphiles which are assumed to be identical. The free energy of swelling (of a fluid phase of the copolymer) ΔF_{sw} is then given by

$$\Delta f_{\text{sw}}/kT = \frac{1}{1+m} \ln \frac{1}{1+m} + \frac{m}{1+m} \ln \frac{m}{1+m} + \frac{3}{2} \left(\frac{l_0}{R_0} \right)^2 m \quad (9)$$

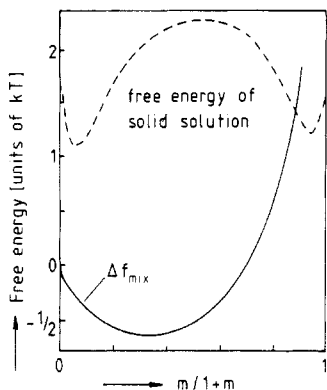


Figure 11. Plot of free energy change f_{sw} (per hydrophilic chain and in units of kT) associated with the swelling of the copolymer. The dashed curve corresponds to the molar free energy of the crystalline mixture (which is lowered at increasing lateral pressure). Note that $m/(1+m)$ is the molar fraction of the monomeric lipid.

In Figure 11 Δf_{sw} is plotted for a value of $l_0^2 = 80 \text{ \AA}^2$ and $R_0^2 = 200 \text{ \AA}^2$ (R_0^2 equal to area A_{on} of pressure onset) as a function of the molar fraction of monomers. The minimum corresponds to the saturation limit. Of course, further addition of monomers will not lead to a lateral phase separation on a macroscopic scale. It is, however, possible that the monomer forms small micropatches. However, a small excess attraction between the two types of surfactants could change the situation drastically by leading to a free energy curve with a double minimum resulting in lateral phase separation also in the fluid state.

An important feature of the free energy curve is the sharp rise at high monomer concentrations because it causes a crossover of the Δf_{sw} curve with the free energy of the crystallization mixture if the lateral pressure approaches the transition pressure of the pure DMPE. Then the mixture decomposes into a crystalline phase of nearly pure DMPE and a slightly oversaturated gel phase. It is for this reason that the DMPE in the mixture crystallizes at practically the same pressures as in the pure lipid monolayer.

The adsorption energy (f_{ad} in eq 1) increases less strongly with m than does the elastic energy ($f_{ads} \propto -(1+m)^{3/4}$); it will therefore only shift the minimum and the sharp uprise of Δf_{sw} to somewhat higher m values. The situation would, however, change dramatically if a certain fraction of the monomer and the hydrophilic chains would become oppositely charged. Then the attraction energy contributing to Δf_{sw} would increase with increasing monomer concentration up to a saturation point. The swelling energy Δf_{sw} would exhibit a double minimum and one would observe phase separation. This is an interesting situation because it is encountered in cell plasma membranes such as the red blood cell where the spectrin filaments are coupled to the partially charged lipid bilayer. This point will be discussed in the Conclusions section.

Formation of Two-Dimensional Foamlike State at $A > A_{on}$. Insoluble surfactant molecules do not spread completely at low densities ($A > A_{on}$), forming a two-dimensional gas, but exhibit a foamlike (or vaporlike) state composed of a coexisting condensed and an expanded (gas) phase. The density of the former is equal to the fluid phase at $A \approx A_{on}$. The foam formation is also the reason for the finding that the pressure becomes suddenly very small at $A = A_{on}$. Convincing evidence for the foamlike states comes from recent microfluorescence studies.^{23c,24c}

The formation of a foamlike state instead of a two-dimensional gas can also be understood in terms of the scaling law approach. Since it is found for all lipids (also

such with small head groups), it is essentially a consequence of the interaction of the hydrophobic chains with the air/water interface. Although these are rather short ($N \approx 15$), we assume that the scaling description can be applied to the very flexible hydrocarbon chains (persistence length of order of monomer diameter) as suggested by Alexander.²²

The free energy of a highly diluted collection of surfactants on the air/water interface is determined by the following contributions: (1) The free translational energy $f_{tr} = kT \ln A$ (A area per lipid). (2) The hydrophobic interaction of the chains with the water surface. This corresponds to a repulsive adsorption energy that is a positive value of δ in eq 1. According to critical micelle concentration studies, the hydrophobic interaction energy per CH_2 is about $\delta = 2kT$.²⁸ (3) The mutual interaction of the hydrophobic monomers. Due to the low density of air it is supposed to behave as a poor solvent, so that the monomer interaction becomes attractive at the low densities considered here. In the Flory-Huggins approach this is accounted for by a negative Flory parameter ν .⁴ (4) The confinement energy. In order to simplify the discussion the free confinement energy of an ideal chain is considered below instead of the expression of eq 3.

The second and third contributions strongly favor a condensation of the surfactants, while the first term acts in favor of the gaslike state. The total free energy per hydrophobic chain is then given by

$$\frac{1}{kT}(f - f_0) \approx N\delta\left(\frac{a}{D}\right) - \frac{N^2|\nu|}{AD} + N\frac{a^2}{D^2} + \ln A \quad (10)$$

The free energy can be expressed in terms of the area per head group A by minimizing $f - f_0$ with respect to D and by inserting the optimal D value into eq 10.

The free energy per chain is then given by

$$f = f_0 - kTN\delta - kT\frac{N|\nu|}{A} + kT \ln A \quad (11)$$

f_0 includes the interaction of the head groups with the surface and the repulsion between the head groups which depends also on A . It is, however, a weak interaction in the low-density limit and is therefore neglected. The free energy is a nonmonotonic function with a maximum at a molar area of about $A_0 \approx Na^2$ for $\delta \approx 1$ and minima at $A \rightarrow \infty$ and $A \rightarrow 0$. At low molecular densities ($A \approx 300 \text{ \AA}^2$) a phase instability and decomposition into a condensed and a gaslike phase is therefore indeed predicted by the scaling law approach.

Conclusions

The polymeric lipids of the type studied in the present work seem to be more suited for the preparation of models of cell plasma membrane than normal polymerized amphiphiles. There exist, for instance, some analogies of the copolymers to the spectrin/actin network coupled to the inner monolayer of the plasma membrane of the red blood cell, the so-called cytoskeleton.

The major component of this network is spectrin, a filamentous protein dimer of 1000- \AA contour length, which exhibits the following special features: First, spectrin is quite flexible and is thus expected to be substantially folded. Second, two filaments are interconnected at one end by an actin oligomer, whereas the other ends are attached to an integral protein of the membrane (the so-called band III protein). This is analogous to the coupling of the amphiphilic chains of the copolymers to the lipid molecules. Third, the spectrin filaments are cross-linked

by the actin oligomers, thus forming a quasi-two-dimensional network. Finally, recent model membrane experiments in the Munich laboratory provided evidence that the spectrin filaments adsorb to the negatively charged lipid component, the phosphatidylserine of the inner monolayer of the plasma membrane (comprising about 20% of the total lipid). By the introduction of (1) amphiphiles with more than one functional group per polar head and (2) partially charged hydrophilic chains, the last two features of the cytoskeleton could be mimicked as well.

Most probably, the spectrin filaments are also partially stretched owing to the separation of the anchoring points (the band III molecule) by the lipid and the electrostatic coupling of the (folded) chains to the bilayer. They act as entropy springs. For that reason it has been postulated that the spectrin/actin meshwork behaves as an ionic gel and that the shape and the deformability of the red blood cell are determined primarily by its shear elastic properties.³⁰ The partial stretching of the chains by the lipids should also lead to saturation behavior at a certain lipid-to-spectrin ratio. This is interesting from the point of view of the evolution of the cytoskeleton of the maturing cells. Recent experiments by Lazarides and Moon³¹ suggest that the cytoskeleton evolves by successive addition of spectrin to the lipid/protein bilayer of the plasma membrane until saturation is reached, after which the nucleus is expelled.

Many of the physical properties of the monomolecular films of the copolymer and of its mixtures with monomers can be explained in terms of the scaling concept of adsorbed macromolecules, so that systems as studied here may provide interesting models to test scaling laws.

Of special technical interest is the demonstration that compound monolayers of polymerized and monomeric lipid patches may be deposited onto solid substrates. This is of interest from the point of view of the preparation and stabilization of Langmuir-Blodgett films containing membrane proteins since the latter can only be incorporated into fluid phases. The polymerized domains can serve to stabilize the films. Proteins have been successfully incorporated in partially polymerized vesicles.¹⁶

Acknowledgment. This paper was written during a visit by one of the authors (E.S.) in the laboratory of Prof. Evan Evans at the Department of Pathology of the University of British Columbia, Vancouver, Canada. Many helpful discussions with Prof. Evans are most gratefully acknowledged. Moreover, we are grateful for financial support by the Deutsche Forschungsgemeinschaft (Sa 246-16/1) and the Fonds der Chemischen Industrie.

Registry No. DMPE, 20255-95-2; *m*-(4,16)-POMEYC, 96326-73-7; *p*-(4,16)-POMEYC, 105473-55-0; CO-I,1 (copolymer), 105473-59-4; CO-II,1 (copolymer), 106906-20-1.

References and Notes

- (1) Sackmann, E.; Eggl, P.; Fahn, C.; Bader, H.; Ringsdorf, H.; Schollmeier, M. *Ber. Bunsen-Ges. Phys. Chem.* **1985**, *89*, 1198.
- (2) Sackmann, E.; Duwe, H. P.; Engelhardt, H. *Faraday Discuss.* **1986**, *81*, 0000.
- (3) Evans, E. A. *Biophys. J.* **1974**, *14*, 923.
- (4) de Gennes, P.-G. *Scaling Concepts in Polymers Physics*; Cornell University: Ithaca, NY, 1953.
- (5) Roberts, G. G. *Contemp. Phys.* **1984**, *25*, 109.
- (6) Sugi, M. *J. Mol. Electron.* **1985**, *1*, 3.
- (7) Sackmann, E.; Frey, W.; Schneider, J., to be published.
- (8) Kuhn, H.; Möbius, D.; Bücher, H. In *Physical Methods of Chemistry*; Weissberger, A., Rossiter, B. W., Eds.; Wiley: New York, 1972; Vol. I, p III B 57.
- (9) Johnston, D. S.; Chapman, D. *Biochemistry* **1983**, *22*, 3194.
- (10) Kunitake, T.; Kimizuka, N.; Higashi, N.; Nakashima, N. *J. Am. Chem. Soc.* **1984**, *106*, 1978.
- (11) Regen, S. L. *Macromolecules* **1983**, *16*, 335.
- (12) Schneider, J. Diploma Thesis, 1985, Mainz.
- (13) Kunitake, T.; Nakashima, N.; Takarabe, T.; Nagai, M.; Tsuge, A.; Yanagi, H. *J. Chem. Soc.* **1981**, *103*, 5945.
- (14) Elbert, R.; Laschewsky, A.; Ringsdorf, H. *J. Am. Chem. Soc.* **1985**, *107*, 4134.
- (15) Wagner, N.; Dose, K.; Koch, H.; Ringsdorf, H. *FEBS Lett.* **1981**, *132*, 313.
- (16) Büschl, R.; Folda, Th.; Ringsdorf, H. *Makromol. Chem. Suppl.* **1984**, *6*, 245.
- (17) Johnston, D. S.; Sanghera, S.; Manjon-Rubin, A.; Chapman, D. *Biochim. Biophys. Acta* **1980**, *602*, 213.
- (18) Fendler, J. H.; Tundo, P. *Acc. Chem. Res.* **1984**, *17*, 3-8.
- (19) Wegner, G. *Makromol. Chem.* **1972**, *154*, 35.
- (20) Daoud, M.; de Gennes, P.-G. *J. Phys.* **1977**, *38*, 85-93.
- (21) de Gennes, P.-G. *J. Phys.* **1976**, *37*, 1445-1452.
- (22) Alexander, S. *J. Phys.* **1977**, *38*, 983-987.
- (23) (a) Fischer, A.; Sackmann, E. *J. Phys.* **1984**, *45*, 517. (b) Fischer, A.; Sackmann, E. *Nature (London)* **1985**, *313*, 299. (c) Fischer, A.; Sackmann, E. *J. Colloid Interface Sci.* **1986**, *112*, 1.
- (24) (a) Albrecht, O.; Gruler, H.; Sackmann, E. *J. Colloid Interface Sci.* **1980**, *79*, 319. (b) Albrecht, O. *Thin Solid Films* **1983**, *99*, 227. (c) Lösche, M.; Sackmann, E.; Möhwald, H. *Ber. Bunsenges. Phys. Chem.* **1984**, *87*, 848.
- (25) The following abbreviations are used: DMPC, dimyristoylphosphatidylcholine; DMPE, dimyristoylphosphatidylethanolamine; (4,16)-POMEYC, sodium bis(hexadecyloxy)propyl 12-methacryloyl-3,6,9,12-tetraoxadodecyl phosphate.
- (26) Rieke, W. D. *Optik* **1962**, *19*, 273.
- (27) In the case of transfer from the fluid-solid coexistence region, the diffraction pattern of the platelets often vanishes within seconds after focusing the electron beam for observation even in the low-dose mode of the EM 400 T. In contrast, the diffraction pattern can be observed for several minutes before a remarkable radiation damage occurs if monolayers are deposited from the completely condensed state (≥ 30 mN m⁻¹). This is explained in terms of a much higher defect density in the former case.
- (28) Adamson, A. W. *Physical Chemistry of Surfaces*, 2nd ed.; Interscience: New York, 1967; p 411.
- (29) Tanford, Ch. *The Hydrophobic Effect*; Wiley: New York, 1973.
- (30) Stokke, B. T.; Mikkelsen, A.; Elgsaeter, A. *Eur. Biophys. J.* **1986**, *13*, 203-218.
- (31) Lazarides, E.; Moon, R. T. *Cell (Cambridge, Mass.)* **1984**, *37*, 354.